Carbohydrate Polymers 97 (2013) 210–216

Contents lists available at SciVerse ScienceDirect

Carbohydrate Polymers

journal homepage: www.elsevier.com/locate/carbpol

Aminoalcohol functionalized zirconium phosphate as versatile filler for starch-based composite membranes

Monica Pica*, Anna Donnadio, Valentina Bianchi, Sacha Fop, Mario Casciola

Perugia University, Department of Chemistry, Via Elce di Sotto 8, 06123 Perugia, Italy

ARTICLE INFO

Article history:
Received 21 December 2012
Received in revised form 24 April 2013
Accepted 25 April 2013
Available online 1 May 2013

Keywords:
Starch
Zirconium phosphate
Aminoalcohol
Composite membrane
Mechanical properties
Water uptake

ABSTRACT

Microcrystalline zirconium phosphate was exfoliated by treatment with aqueous solutions of α,ω-alkylaminoalcohols and employed for the fabrication of potato starch composite membranes. Glycerol-based and glycerol-free composite membranes, containing 5 wt% of filler, were prepared from gelatinized starch and characterized for their physico-chemical properties. Despite of a partial filler reaggregation, as revealed by XRD and SEM analysis, all the composites exhibited a significant increase in the Young's modulus with respect to the glycerol-starch membrane, up to 80% and 190% for the glycerol-based and the glycerol-free composites, respectively. For both kinds of membranes the filler delays to a large extent the starch decomposition above about 300 °C. A significant reduction in the water uptake of the composites was also observed with respect to the neat glycerol-based membrane, up to about 70% for the glycerol-free composites.

1. Introduction

Starch is an agricultural feedstock biopolymer found in a variety of plants. Its granules are actually formed by one branched (amylopectin) and one linear (amylose) polymer. It can be used as a natural filler material in the form of granules which can be incorporated into synthetic plastic matrices as rapidly biodegradable components (Kolybaba et al., 2003), or as biodegradable matrix, for the production of plastic materials. Starch-based plastics often contain glycerol or similar hydrophilic organic molecules, which are used as plasticizers to increase softness and pliability, but reducing, at the same time, mechanical strength and moisture stability (Talja, Helen, Roos, & Jouppila, 2007; Vieira, da Silva, dos Santos, & Beppu, 2011). Several examples in the literature report an improvement of the mechanical stability of plasticized starch films by incorporation of inorganic fillers, among which layered materials such as clays and zirconium phosphates (ZP) and phosphonates (Donnadio, Pica, Taddei, & Vivani, 2012; Pica, Donnadio, & Casciola, 2012). More specifically, recent works demonstrated that high aspect ratio ZP particles allow to improve the mechanical strength and to reduce the water uptake of glycerol-plasticized potato starch films (Pica et al., 2012), while zirconium phosphonate particles, bearing hydroxyalkyl amino phosphonic groups covalently bonded to the inorganic layers, allow to obtain flexible starch films without using any plasticizing agent and exhibiting superior mechanical and thermal properties with respect to glycerol-starch films (Donnadio et al., 2012). Both these approaches exhibit advantages and drawbacks. On one hand ZP results to be an extremely versatile filler, since it is possible to effectively control the particle morphology, in particular the aspect ratio, by a suitable selection of the starting materials; on the other hand, due to the stiffness of the ZP particles, the use of plasticizing agents, such as glycerol, is generally required for the preparation of starch-based films. Differently, zirconium hydroxyalkyl amino phosphonates turned to be able to act both as reinforcing agent and as plasticizers for the starch matrix, allowing to obtain resistant films with good plastic properties; at the same time, the difficulty to control the morphology of the zirconium phosphonate particles did not allow to obtain a good degree of dispersion of the filler and, then, to reduce its loading within the starch matrix. Taking into account these considerations, it seemed of interest to combine the advantages deriving from the use of an extremely versatile filler, such as ZP, with those arising from the presence of organic species which should be able to interact with both ZP and starch, in order to obtain new glycerol-free starch composites.

In the present work, high aspect ratio ZP particles functionalized with aliphatic α,ω-aminoalcohols ($NH_2(CH_2)_nOH$, $n = 3–6$, hereafter indicated as C_n) were used as fillers for a potato starch matrix. Differently from the previous work, in which the aminoalcohol functionalities were covalently anchored to the inorganic layer starting from preformed hydroxyalkyl amino phosphonates, in this case aminoalcohol functionalized ZP was obtained through

* Corresponding author. Tel.: +39 075 585 5564; fax: +39 075 585 5566.
E-mail address: monica.pica@unipg.it (M. Pica).

0144-8617/$ – see front matter © 2013 Elsevier Ltd. All rights reserved.
http://dx.doi.org/10.1016/j.carbpol.2013.04.078

a simpler and more versatile synthetic approach based on the aminoalcohol intercalation into preformed ZP. The aminoalcohol molecules, which are bonded to the ZP layers through ionic interactions involving the $-PO^-$ and the $-NH_3^+$ groups, are expected to act both as compatibilizers and as plasticizers for the polymer matrix through the hydroxyl groups which should form hydrogen bonds with the starch—OH groups. In order to investigate the ability of aliphatic aminoalcohols to act also as plasticizers for the starch matrix, glycerol-free starch membranes containing functionalized ZP particles were prepared, together with glycerol-based composites. The samples were characterized by structural, morphological and thermal analysis, mechanical tests and water uptake measurements.

2. Experimental

2.1. Materials

Native potato starch (amylose about 20%, amylopectin about 80%) was kindly supplied by Novamont. Zirconyl propionate ($ZrO_{1.27}(C_2H_5COO)_{1.46}$, MW = 218 Da) was supplied by MEL Chemicals, England. All other reagents were supplied by Aldrich.

2.2. Preparation of α-$Zr(HPO_4)_2·H_2O$ (ZP)

Microrystalline α-$Zr(HPO_4)_2·H_2O$, consisting of platelets with an average planar size of 2-3 μm, was prepared as reported by Capitani, Casciola, Donnadio, and Vivani (2010). 0.88 g of zirconyl propionate was solubilized, under stirring at room temperature, in 35 mL of an aqueous solution of oxalic acid so that the Zr(IV) concentration was 0.1 M and the $H_2C_2O_4$/Zr molar ratio was 10. Then 1.43 mL of 14.8 M H_3PO_4 was added so that the H_3PO_4/Zr molar ratio was 6. The resulting solution was heated for 24 h at 80 °C in a closed plastic bottle. The precipitate thus obtained was separated from the solution by centrifugation at 3000 rpm, washed three times with 10^{-3} M HCl, dried overnight at 80 °C, and finally kept in a desiccator over a saturated $Mg(NO_3)_2·6H_2O$ solution (53% relative humidity,RH).

2.3. Preparation of the colloidal dispersions of ZP and α,ω-alkylaminoalcohols (C_n, n = 3–6)

Four colloidal dispersions of ZP containing the same amounts of C_n were prepared as follows: 0.25 g of microcrystalline ZP was suspended in 16.3 mL of deionised water. Then, 8.6 mL of a 0.1 M solution of C_n was added dropwise and under vigorous stirring to the previous suspension, so that the C_n/Zr molar ratio was 1. Colloidal dispersions of ZP·C_n (hereafter ZP·C_n), were obtained and left under stirring for 24 h. In order to prove that the aminoalcohol molecules are quantitatively taken up by ZP, the pH of both C_n solutions and ZP·C_n dispersions was measured. As an example, the pH of the 0.1 M C_3 solution was 10.7, while that of the dispersions obtained after the reaction of ZP with C_3 was 6.5 ± 0.2 and in all cases was in the range 6-7, thus indicating that the fraction of neutral C_n molecules in the solution is negligible.

2.4. Preparation of the composite starch membranes containing ZP·C_n

Starch films, plasticized with glycerol, containing 5 wt% ZP·C_n (hereafter GS/ZP·C_n) were prepared as follows. One gram of NS was dispersed in 25 mL of water and heated at 90 °C for 10 min until gelatinization occurred. A weighed amount of the ZP·C_n dispersion was added to the starch gelatine and the mixture was left at 90 °C under stirring for 20 min; then a glycerol amount of 0.25 g was added to the previous mixture and left at 90 °C under stirring for 20 min. The final dispersion was cast on a polystyrene dish and left in an oven at 40 °C overnight.

By using the same kind of procedure a starch/glycerol film (hereafter GS), a glycerol free starch film (S) and glycerol-free composite starch films containing the same amount of ZP·C_n per gram of starch were also prepared: these composites will be hereafter indicated as S/ZP·C_n. Due to its high rigidity and brittleness, which hampered the film handling, the S sample was used only to compare the structural and thermal properties. All films were 95–105 μm thick.

2.5. Techniques

2.5.1. X-ray diffraction

X-ray diffraction patterns of powders and cast films were collected with a Philips X-Pert powder diffractometer, a PW3020 goniometer equipped with a bent graphite monochromator on the diffracted beam, a PW3011 detector using the Cu-*K*α radiation source with 2θ step size of 0.030° and step scan of 0.5 s. The LFF ceramic tube operated at 40 kV, 30 mA.

The crystallite size (t), along the c-axis, were determined applying the Scherrer equation, $t = K\lambda/\beta\cos\theta$, in which K was set to 0.9, and λ = 1.5406 Å. The integral breadths of the (0 0 2) peaks, β, were evaluated for all the samples by fitting the peaks with a pseudo-Voigt function, and corrected for the instrumental broadening contribution, that was previously evaluated by the Rietveld refinement of the profile of lanthanum hexaboride, LaB_6, as external peak profile standard. LaB_6 was provided by The Gem Dugout–Deane K. Smith, 1652 Princeton Drive, State College, PA 16803.

2.5.2. Thermogravimetric analysis

Thermogravimetric determinations were carried out by a NETZSCH STA 449 Jupiter thermal analyser connected to a NETZSCH TASC 414/3 A controller at a heating rate of 10 °C/min, with an air flow of about 30 mL/min. Before measurements, all samples were equilibrated at 33% R.H.

2.5.3. SEM analysis

Scanning electron microscopy (SEM) images were collected by a Zeiss LEO 1525 FE SEM. The composite films were fractured in liquid N_2. All samples were coated with a thin layer of carbon before SEM observation.

2.5.4. Mechanical tests

Mechanical tests were carried out by a Zwick Roell Z1.0 testing machine, with a 200 N static load cell. Young's modulus (slope of stress–strain curve at low values of strain), tensile strength (maximum force used during measurement) and elongation at break (ratio of elongation to original length of sample at break) were measured on rectangle shaped film stripes, obtained by a cutting machine, length and width of which were 100 mm and 5 mm, respectively. Before testing, samples were equilibrated for 7 days in vacuum desiccators at 33% RH and room temperature (20–23 °C) and the thickness of the film stripe, determined with an uncertainty of ±5 μm, was in the range 95-105 μm. An initial grip separation of 10.000 ± 0.002 mm and a crosshead speed of 5 mm/min was used. All tests were carried out at room temperature (20–23 °C). Both the uncertainty, deriving from the sample size determination, and the standard deviation, resulting from the analysis of five film stripes for each sample, were considered for statistical analysis. The data were elaborated by the TestXpert V11.0 Master software.

2.5.5. Water vapour uptake

The samples were dehydrated over P_2O_5 before being conditioned in the presence of water vapour. Then, films were equilibrated, at room temperature, at 90% RH for one week. The water uptakes (%w.u.) were calculated from the increase in mass

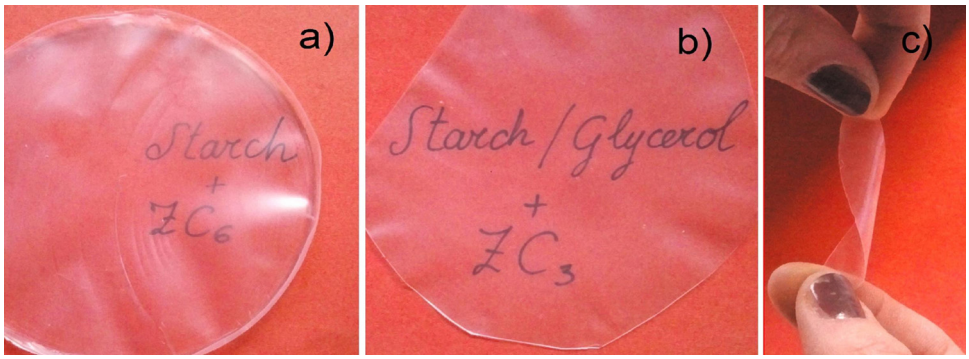

Fig. 1. Images of an S/ZP·C_6 (a and c) and a GS/ZP·C_3 (b) membrane.

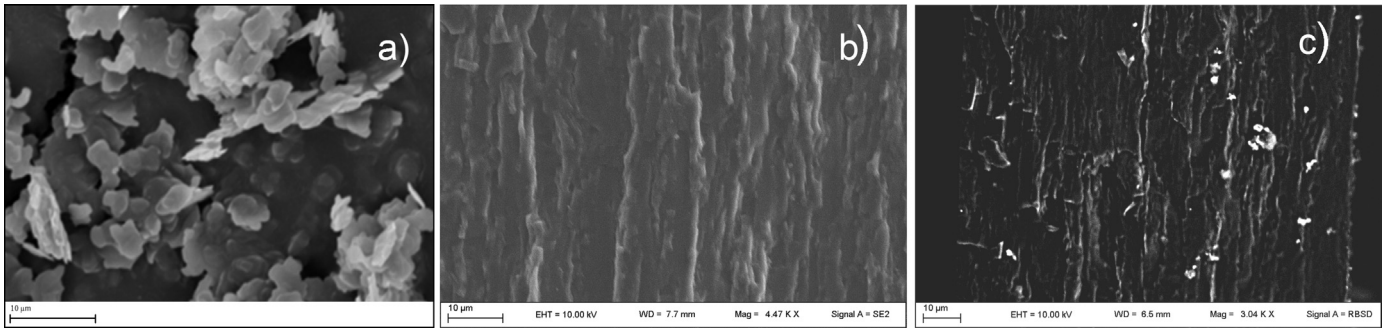

Fig. 2. SEM image of pristine ZP (a); a GS/ZP·C_3 membrane collected with secondary (b) and backscattered (c) electrons.

of the dried samples (Chung et al., 2010), by using the following equation:

$$\%\text{w.u.} = \frac{w_{90} - w_{an}}{w_{an}} \times 100$$

where w_{90} is the weight of the samples equilibrated at 90% RH, w_{an} is the weight of the samples dehydrated over P_2O_5.

3. Results and discussion

It is well known that the presence of HPO_4 groups in ZP allows the exchange of the proton with a large variety of cationic species, even organic cations (Clearfield & Costantino, 1996), as well as the intercalation of basic molecules in the interlayer region. As a matter of fact, when an aqueous propylamine (Pr) solution is added dropwise to a ZP suspension, a transition from a two-phase (ZP and water) to a one-phase system (ZP·Pr dispersion in water) is observed. Since propylamine intercalation leaves the ZP layers unaltered, it was concluded that this dispersion originates from ZP exfoliation, leading to the formation of very thin particles made of single lamellae or packets of few ZP layers (Alberti, Casciola, & Costantino, 1985), having an aspect ratio higher than that of the pristine ZP.

In the present work four colloidal ZP·C_n dispersions have been prepared by using aqueous C_n solutions, with $n = 3$–6: the aminoalcohol molecules are quantitatively taken up by ZP (Benes, Melanova, Zima, Patrono, & Galli, 2003) and promote the layer separation. Although quantitative information on the exfoliation degree of ZP·C_n is not available, it can be considered that, similarly to ZP·Pr dispersions (Casciola et al., 2005), the treatment of ZP·C_n dispersions with 1 M HCl solution leads to the regeneration of the amorphous H^+-form of ZP. This suggests a high degree of ZP·C_n exfoliation which, due to the fast layer reaggregation, gives rise to the formation of amorphous ZP.

The ZP·C_n colloidal dispersions were used to prepare two series of composite potato starch membranes by solution casting: the first series (hereafter S/ZP·C_n) did not contain any organic plasticizer, while the second series of membranes (hereafter GS/ZP·C_n) contained also 25 wt% of glycerol with respect to starch. In order to verify the stability of the ZP·C_n dispersions in the same conditions employed for the membrane fabrication, both C_n solutions and ZP·C_n dispersions were heated at 90 °C for at least 20 min and then the pH was measured. As an example, the pH of the hot ZP·C_3 dispersion was 6.2 ± 0.2, while the pH of the hot C_3 solution was 9.9 ± 0.2, thus proving that the aminoalcohol molecules remain anchored to the ZP layers and that the fraction of neutral C_3 molecules in the solution is negligible also in these conditions. Similar results were obtained for the other ZP·C_n dispersions and C_n solutions.

Fig. 1a shows an S/ZP·C_6 membrane, while Fig. 1b shows a GS/ZP·C_3 membrane. Both membranes appear macroscopically homogeneous and transparent. Moreover, Fig. 1c shows that the sample S/ZP·C_6 exhibits also a good flexibility, even though it does not contain glycerol. This is a remarkable result, especially if one considers that starch membranes filled with naked ZP particles, as well as starch membranes containing the same amount of C_n employed for the S/ZP·C_n composites, turned to be highly brittle and hard to handle. These findings indicate that the flexibility of the S/ZP·C_n composites is due to the simultaneous presence of the inorganic nanoparticles and C_n molecules anchored on their surface, so that the filler plays to some extent the same role as glycerol and can be considered as a solid plasticizer of the starch matrix.

3.1. Electron microscopy analysis

Fig. 2a shows the SEM image of the ZP pristine material used in the present work, consisting of aggregates of thin platelets with an average planar size of 2-3 µm. Fig. 2b and c show the SEM images of a GS/ZP·C_3 membrane. The image collected with secondary electrons (Fig. 2b) shows a dense and homogeneous matrix, indicating

Table 1
Interlayer distances, in Å, for ZP·C_n intercalation compounds, S/ZP·C_n and GS/ZP·C_n composites, compared with those reported in the literature (Benes et al., 2003) for Phase 1 of amino alcohol intercalated ZP.

n	ZP·C_n	S/ZP·C_n	GS/ZP·C_n	Phase 1
3	11.6	11.7	11.6	11.7
4	12.0	11.8	11.8	12.0
5	13.5	13.5	13.3	13.8
6	14.5	14.3	14.3	14.3

Table 2
Average thickness of the crystalline domains of ZP·C_n in the GS/ZP·C_n and GS/ZP·C_n composites.

Sample	t_1 (nm)	Sample	t_2 (nm)
GS/ZP·C_3	11	S/ZP·C_3	14
GS/ZP·C_4	12	S/ZP·C_4	14
GS/ZP·C_5	27	S/ZP·C_5	34
GS/ZP·C_6	53	S/ZP·C_6	32

that the native starch granules were destroyed and formed a continuous phase with glycerol. The image collected in backscattering (Fig. 2c) reveals the presence of bright spots due to micrometric and submicrometric filler aggregates dispersed within the polymer matrix, indicating that the filler is present in a partially aggregate state.

3.2. X-ray diffraction analysis

Fig. 3 displays the X-ray diffraction patterns of GS/ZP·C_n (A) and S/ZP·C_n (B) samples. The patterns of all composites show reflections at low 2θ values that do not appear in the pattern of starch. These reflections, ascribed to the stacking of the α-layers of ZP·C_n, were also observed in the X-ray patterns of the solids obtained by heating to dryness the ZP·C_n dispersions under the same conditions used for the membrane preparation. Moreover, the interlayer distances associated with these reflections (Table 1) are nearly coincident with the interlayer distances of ZP intercalation compounds containing one aminoalcohol per Zr atom (Phase 1 of Benes et al., 2003). Besides the peak of the Phase 1, the X-ray patterns of GS/ZP·C_4 and S/ZP·C_4 (Fig. 3, curves (b)) show an additional peak which, according to Benes et al., is characteristic of an intercalation compound having composition $Zr(HPO_4)_2 \cdot 0.5C_4$. All these findings show that, when the solvent is removed from the polymer–filler dispersions, the filler tends to reaggregate with formation of crystalline domains of aminolacohol intercalated ZP, without co-intercalation of starch and/or glycerol.

It is also noteworthy that the patterns of the composite films only show the reflections due to the (0 0 2) crystallographic planes of the filler, thus indicating that the intensity of these reflections is significantly affected by preferred orientation of the lamellar filler parallel to the film surface. It must also be recalled that preferred orientation effects generally increase with increasing the particle aspect ratio (Capitani et al., 2010): specifically, the planar size of the layers being the same, preferred orientation is expected to increase with decreasing the thickness of the crystalline domains along the layer packing direction. In the presence of these effects, it is not possible to quantify the degree of filler aggregation by X-ray analysis. However, some general considerations can be done by evaluating the following parameters that are obtained from the analysis of the (0 0 2) reflection of the X-ray patterns:

- the average thickness of the filler crystalline domains (hereafter indicated as t), along the direction of layer packing, for the GS/ZP·C_n (t_1) and the S/ZP·C_n (t_2) samples;
- the area of the (0 0 2) reflection, hereafter indicated as A_1 for the GS/ZP·C_n and as A_2 for S/ZP·C_n.

Since the X-ray patterns of GS/ZP·C_4 and S/ZP·C_4 showed the presence of two (0 0 2) reflections having area A_a and A_b, corresponding to two crystalline domains having thickness t_a and t_b, the weighted average of the crystallite thickness was considered and calculated as follows:

$$t = (t_a A_a + t_b A_b)/(A_a + A_b)$$

The total area of the two peaks ($A_a + A_b$) in GS/ZP·C_4 and S/ZP·C_4 was instead considered for the calculation of A_1 and A_2.

Table 2 reports the average thickness of the crystalline domains of ZP·C_n in the glycerol-based and glycerol-free composites. In both series of membranes the crystallite size increases with increasing the alkyl chain length of the aminoalcohol, especially in the presence of glycerol. This is probably due to the fact that, with increasing the alkyl chain length, chain–chain interactions become progressively more intense and promote layer aggregation. In support of this hypothesis there is the fact that a similar increase in the crystallite thickness was observed for the dried ZP·C_n dispersions with increasing the aminoalcohol chain length.

To further highlight the filler behavior in the presence and in the absence of glycerol, the A_1/A_2 ratio was plotted as function of n and reported in Fig. 4.

Taking into account that the size of the crystalline domains is nearly independent of the presence of glycerol in the ZP·C_3, ZP·C_4 and ZP·C_5 composites, it can be reasonably assumed that preferred orientation effects are similar in these glycerol-free and glycerol-based composites, so that the evolution of the A_1/A_2 ratio provides reliable information on the relative amount of crystalline phase in the two kinds of composite. Therefore, on the basis of Fig. 4 it is suggested that glycerol does not affect the tendency of ZP·C_3 and ZP·C_4

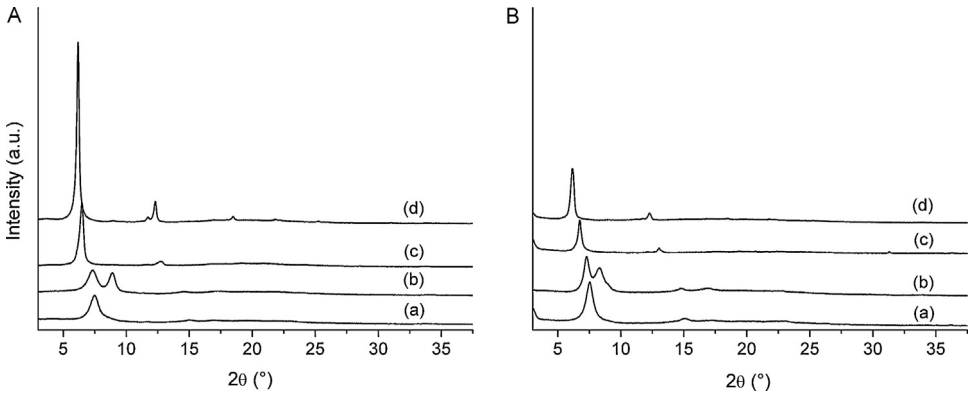

Fig. 3. X-ray diffraction patterns of: (A) GS/ZP·C_3 (a). GS/ZP·C_4 (b), GS/ZP·C_5 (d), GS/ZP·C_6 (d); (B) S/ZP·C_3 (a), S/ZP·C_4 (b), S/ZP·C_5 (d), S/ZP·C_6 (d).

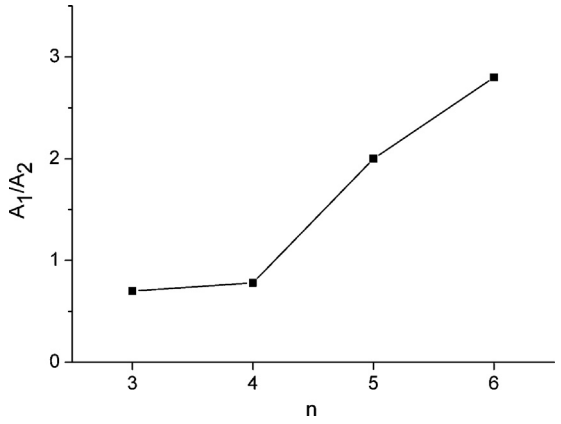

Fig. 4. A_1/A_2 ratio as function of n. A_1 and A_2 are the areas of the (002) reflection of ZP·C_n in GS/ZP·C_n and S/ZP·C_n, respectively.

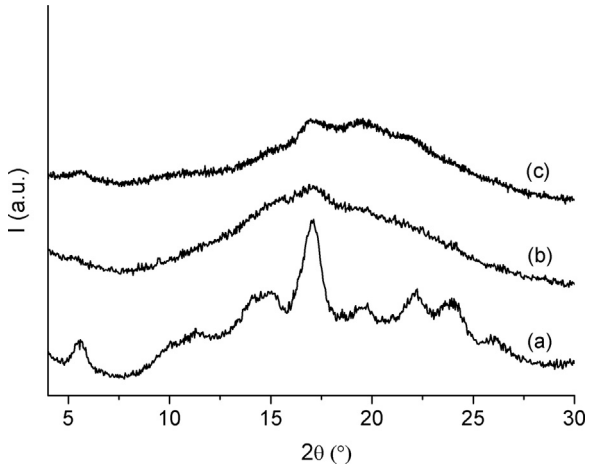

Fig. 5. X-ray diffraction patterns of native starch (a), S (b), GS (c) samples.

to give crystalline aggregates, while it promotes the formation of a larger amount of crystalline phase in the ZP·C_5 composite.

For the composite containing ZP·C_6, the preferred orientation effects are expected to be stronger in the absence of glycerol, as the crystallites are thinner. Nevertheless, the larger peak area was observed in the glycerol-based composite, thus indicating that the fraction of crystalline filler is much higher in GS/ZP·C_6 with respect to S/ZP·C_6.

In conclusion, even if possible effects of preferred orientation are considered, the A_1/A_2 dependence on n indicates that the fraction of crystalline filler in GS/ZP·C_n is about the same as that in S/ZP·C_n for $n = 3$ and 4, but it is larger than that (and increases with n) for $n = 5$ and 6. This is probably due to the fact that glycerol may compete with aminoalcohols in the interaction with starch thus weakening the ZP·C_n–starch interaction and promoting the layer aggregation: consequently, those ZP·C_n compounds where the chain–chain interactions are stronger turn out to be more aggregated in the presence of glycerol.

As far as structural modifications of starch are concerned, Fig. 5 compares the diffraction pattern of native starch powder with the pattern of a membrane obtained from gelatinized starch in water (S) and that of a GS membrane. The broadening and the intensity decrease of the main starch reflection at about 17° 2θ (Cheetham & Tao, 1998) reveals a progressive disruption of the semi-crystalline structure of the native starch granules as a consequence of the thermal treatment in water (pattern b) and the presence of glycerol (pattern c). The presence of the filler does not significantly modify the pattern of gelatinized starch (Fig. 6). For this reason, it was not possible to evaluate the contribution of the polymer–filler interaction in the starch destructuration.

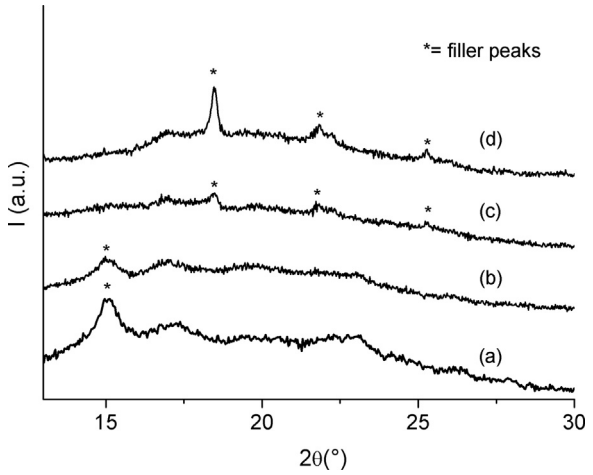

Fig. 6. X-ray diffraction patterns of S/ZP·C_3 (a), GS/ZP·C_3 (b), S/ZP·C_6 (c) and GS/ZP·C_6 (d) samples.

3.3. Thermogravimetric analysis

Thermogravimetric analysis was performed on samples conditioned at 33% RH. The thermogravimetric (TG) profiles of the composite membranes containing ZP·C_3 and ZP·C_6 are compared with those of S and GS samples in Fig. 7. For the sake of clarity the TG curves of all composites are shown separately, together with the corresponding derivatives, in the supporting information. Fig. 7a displays the TG curves of the glycerol-plasticized

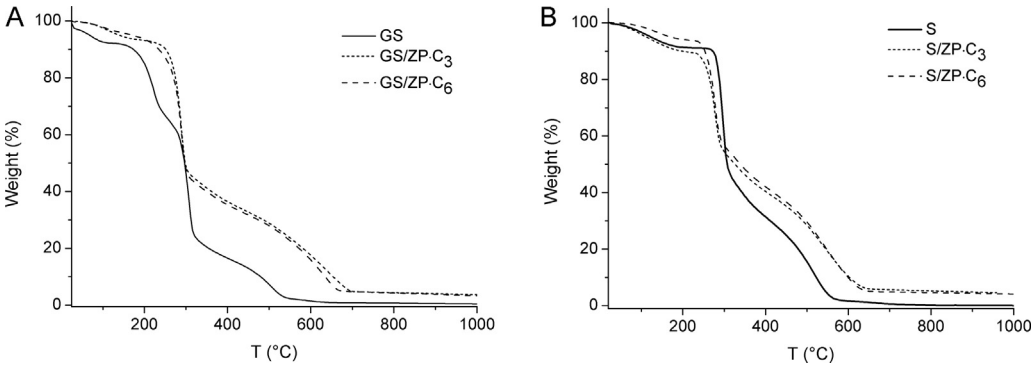

Fig. 7. Thermogravimetric curves of: (A) GS, GS/ZP·C_3, GS/ZP·C_6 and (B) S, S/ZP·C_3, S/ZP·C_6.

Table 3
Young's modulus and tensile strength, at room temperature, of GS/ZP·C_n and S/ZP·C_n samples. The values for $n = 0$ refer to a GS sample.

n	GS/ZP·C_n		S/ZP·C_n	
	Young's modulus (MPa)	Tensile strength (MPa)	Young's modulus (MPa)	Tensile strength (MPa)
0	734 ± 45	17 ± 1	–	–
3	1441 ± 131	38 ± 3	2097 ± 166	66 ± 4
4	1196 ± 69	32 ± 2	2066 ± 115	68 ± 4
5	1261 ± 76	34 ± 3	2263 ± 129	78 ± 4
6	1326 ± 78	33 ± 2	1975 ± 153	54 ± 4

membranes: while the composite membranes exhibit similar profiles, these significantly differ from that of GS.

All the composites show a first weight loss, attributed to the endothermic loss of water, which is smaller and shifted to higher temperatures in comparison with the corresponding loss of GS. After the water loss, the membrane decomposition occurs in three main steps for GS and in only two steps for S and the composites. It can be observed that the second step of the GS sample, centered around 210 °C, is not present in the TG curve of the composites: this step was attributed, in a previous work, to the glycerol loss and to a partial decomposition of the starch matrix (Pica et al., 2012). Thus, in the presence of the filler, the glycerol loss is shifted toward higher temperatures and occurs concomitantly with the starch decomposition. Moreover, also the last step, corresponding to the exothermic decomposition of the starch matrix, is shifted to higher temperatures in the presence of the filler: for example, the temperature corresponding to 80% weight loss increases from 351 °C for GS to about 580 °C for the GS/ZP·C_n composites.

As far as the TG profiles of the glycerol-free samples are concerned (Fig. 7b), it can be observed that the curves of the composites are very close to those of the corresponding glycerol-based samples. On the other hand, the curve profile of S significantly differs from that of GS, being close to that of the composite samples, with three main decomposition steps. While the second step results to be anticipated in the presence of the filler of about 20 °C, the final degradation of the starch in the composites is shifted of about 76 °C toward higher temperatures with respect to neat starch. The fact that the TG curves of the glycerol-based composites are very similar to those of the glycerol-free composites clearly indicates that the filler allows to fully preserve the thermal stability of the neat starch matrix even in the presence of glycerol.

3.4. Mechanical properties

The mechanical tests were performed at room temperature on samples previously conditioned at 33% RH for at least one week. Fig. 8a and b display the stress–strain curves of the GS/ZP·C_n and S/ZP·C_n samples, respectively, together with that of GS. The mechanical properties of the S sample could not be determined because of its rigidity and brittleness which hampered the film handling.

For each test, the stress–strain curve with the greatest elongation at break was chosen since it is representative of the specimen with less macroscopic defects. The GS sample exhibits the typical behavior of ductile polymers: after reaching the yield point, the stress gently drops to the draw stress and remains constant until rupture, while the neck propagates along the specimen. For both GS/ZP·C_n and S/ZP·C_n samples, the presence of the inorganic particles modifies the stress–strain curve profile, giving rise to an increase in the slope of the elastic region and in the tensile strength, as well as to a significant reduction in the elongation at break. In addition, the glycerol-based composites exhibit a plastic behavior to some extent, while the glycerol-free composites result to be more brittle.

Table 4
Water uptake, at room temperature and 90% RH, of GS/ZP·C_n and S/ZP·C_n samples. The water uptake for $n = 0$ refers to a GS sample.

n	GS/ZP·C_n	S/ZP·C_n
0	68 ± 7	–
3	43 ± 4	20 ± 2
4	52 ± 5	24 ± 2
5	54 ± 5	19 ± 2
6	46 ± 5	24 ± 2

The mechanical quantities, derived from the analysis of the stress–strain curves, are reported in Table 3. The presence of the filler particles led to an increase in the Young's modulus in both series of samples: this is an expected result, since the rigidity of the inorganic filler is much higher than that of the organic polymer (Fu, Feng, Lauke, & Mai, 2008; Pica et al., 2012). In particular, the average proportional increment of the Young's modulus was about 80% in the presence of glycerol, and 190% in the absence of glycerol. Within the experimental errors, the modulus of the composites can be considered nearly independent of the kind of aminoalcohol. This fact is not surprising, since it is known that the Young's modulus is measured at too low deformation levels to cause interface separation (Fu et al., 2008). A significant improvement of the tensile strength was also found, the average proportional increment being about 100% for the glycerol-based samples and about 290% for the glycerol-free composites. Especially in the absence of glycerol, the high values of the strength of the composite films could be attributed to some extent to the polymer–filler interfacial interaction which plays an important role in the stress transfer (Fu et al., 2008).

Finally, it can be observed that, in spite of the increase in the tensile strength determined by the presence of the filler, the concomitant reduction of the elongation at break results in the reduction of the area under the stress–strain curve, which makes the composite films less though than neat GS. This behavior, which was already observed for glycerol-starch composites containing ZP particles with micrometric planar size (Pica et al., 2012), is typical of polymer matrices reinforced with high aspect ratio layered particles (Shah, Maiti, Jiang, Batt, & Giannelis, 2005).

3.5. Water uptake measurements

One of the main drawbacks of glycerol-starch films is their sensitivity to moisture. Therefore, it seemed interesting to evaluate the effect of the inorganic particles on the water uptake of the starch-based composites. From the data reported in Table 4 one can observe that the water uptake of the polymeric films at room temperature and 90% RH is significantly lower than that of the GS sample.

In particular, the water uptake is reduced on average by 28% for the glycerol-starch composites and by 68% for the glycerol-free samples. It is interesting to observe that the proportional reduction in the water uptake of the glycerol-free composites is about 2.4 times greater than that of the glycerol-based composites and that the same ratio was found between the proportional increase

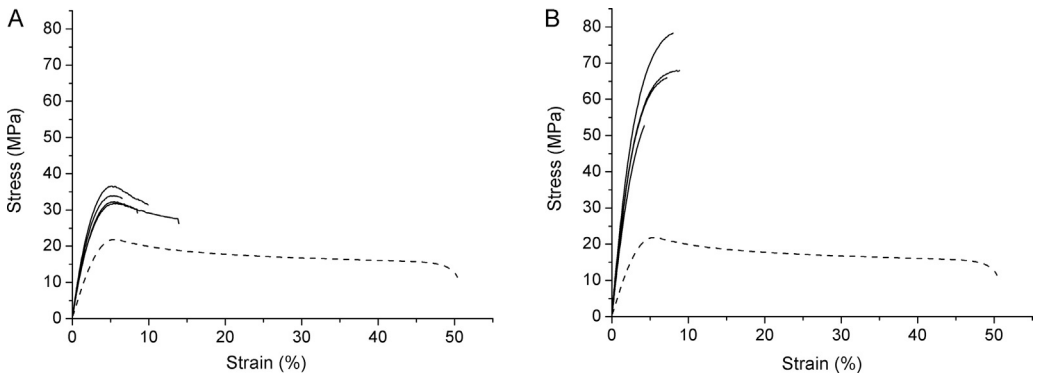

Fig. 8. Stress–strain curves of: (A) GS (dashed line) and GS/ZP·C_n (solid lines); (B) GS (dashed line) and S/ZP·C_n (solid lines).

in the elastic modulus of the two series of the composites: this result suggests that the decrease in the water uptake observed for the composites is strictly connected to the improvement in the mechanical strength of the polymer matrix.

4. Conclusions

Glycerol-based and glycerol-free starch composites containing ZP·C_n were prepared and characterized for their morphological, structural, thermal and mechanical properties. While it was not possible to prepare handable glycerol-free films containing unmodified ZP particles or C_n, the presence of the aminoalcohol modified filler allowed to obtain samples exhibiting a good flexibility and transparency, suggesting that the ZP·C_n acts as a starch plasticizer.

In terms of physical properties, the composite membranes exhibit a better thermal stability than starch especially in the presence of glycerol, a strongly reduced water uptake and a significant improvement of the Young's modulus and tensile strength, which is however associated with a loss of plastic properties.

X-ray diffraction analysis revealed that the dispersion of the filler within the starch matrix was not complete, both in GS/ZP·C_n and S/ZP·C_n composites. In particular, in both series of membranes the crystallite size increases with increasing the alkyl chain length of the aminoalcohol. Moreover, while the amount of crystalline ZP·C_3 and ZP·C_4 is about the same in the glycerol-free and in the glycerol-based composites, it increases in the presence of glycerol for ZP·C_5 and ZP·C_6.

The results reported in this paper suggest that the use, as a filler, of modified ZP particles with organic bases ionically linked on the surface, could offer a suitable and alternative approach to the preparation of starch-based composites since it provides several advantages with respect to the approaches investigated in previous works (Donnadio et al., 2012; Pica et al., 2012).

In particular, the approach here presented combines the possibility to effectively control the morphology of the ZP particles (and therefore to improve the degree of dispersion of the filler within the polymer matrix) with the possibility to choose the ZP functionalizing agent among a large variety of molecules and, consequently, to select those suitable to assure the most effective filler exfoliation and polymer destructuration. Finally, the ability of the phosphate groups to interact with basic molecules through ionic interactions is expected to reduce the leakage of the plasticizing agent, thus improving the stability of the composite.

Acknowledgements

The authors wish to thank Novamont S.p.A. for financial support within the project "Studio, sperimentazione e realizzazione di innovativi nanocompositi plastici biodegradabili a base di olio vegetale e amido nanostrutturato con proprietà meccaniche e funzionali programmate, per la realizzazione di imballaggi ultrasottili" and Dr. Alessandro Di Michele of the LUNA Laboratory, at the Physics Department of Perugia University, for collecting SEM pictures.

Appendix A. Supplementary data

Supplementary data associated with this article can be found, in the online version, at http://dx.doi.org/10.1016/j.carbpol.2013.04.078.

References

Alberti, G., Casciola, M., & Costantino, U. (1985). Inorganic ion exchange pellicles obtained by delamination of a-zirconium phosphate crystals. *Journal of Colloid and Interface Science*, *107*, 256–263.

Benes, L., Melanova, K., Zima, V., Patrono, P., & Galli, P. (2003). Intercalation of amino alcohols into α-$Zr(HPO_4)_2 \cdot H_2O$. *European Journal of Inorganic Chemistry*, *2003*, 1577–1580.

Capitani, D., Casciola, M., Donnadio, A., & Vivani, R. (2010). High yield precipitation of crystalline a-zirconium phosphate from oxalic acid solutions. *Inorganic Chemistry*, *49*, 9409–9415.

Casciola, M., Alberti, G., Donnadio, A., Pica, M., Marmottini, F., Bottino, A., et al. (2005). Gels of zirconium phosphate in organic solvents and their use for the preparation of polymeric nanocomposites. *Journal of Materials Chemistry*, *15*, 4262–4267.

Cheetham, N. W. H., & Tao, L. (1998). Variation in crystalline type with amylose content in maize starch granules: An X-ray powder diffraction study. *Carbohydrate Polymers*, *36*, 277–284.

Chung, Y. L., Ansari, S., Estevez, L., Hayrapetyan, S., Giannelis, E. P., & Lai, H.-M. (2010). Preparation and properties of biodegradable starch–clay nanocomposites. *Carbohydrate Polymers*, *79*, 391–396.

Clearfield, A., & Costantino, U. (1996). Layered metal phosphate and their intercalation chemistry. In G. Alberti, & T. Bein (Eds.), *Two and three-dimensional inorganic networks, comprehensive supramolecular chemistry*. Pergamon, Oxford: Elsevier Ltd. Press [chapter 4]

Donnadio, A., Pica, M., Taddei, M., & Vivani, R. (2012). Design and synthesis of plasticizing fillers based on zirconium phosphonates for glycerol-free composite starch films. *Journal of Materials Chemistry*, *22*, 5098–5106.

Fu, S.-Y., Feng, X.-Q., Lauke, B., & Mai, Y.-W. (2008). Effects of particle size, particle/matrix interface adhesion and particle loading on mechanical properties of particulate – polymer composites. *Composites: Part B*, *39*, 933–961.

Kolybaba, M., Tabil, L. G., Panigrahi, S., Crerar, W. J., Powell, T., & Wang, B. (2003). Biodegradable polymers: present, past, and future. Presented at 2003 CSAE/ASAE Annual Intersectional Meeting, *Paper Number RRV03-0007*.

Pica, M., Donnadio, A., & Casciola, M. (2012). Starch/zirconium phosphate composite films: Hydration, thermal stability, and mechanical properties. *Starch/Starke*, *64*, 237–245.

Shah, D., Maiti, P., Jiang, D. D., Batt, C. A., & Giannelis, E. P. (2005). Effect of nanoparticle mobility on toughness of polymer nanocomposites. *Advanced Materials*, *17*, 525–528.

Talja, R. A., Helen, H., Roos, Y. H., & Jouppila, K. (2007). Effect of various polyols and polyol contents on physical and mechanical properties of potato starch-based films. *Carbohydrate Polymers*, *67*, 288–295.

Vieira, M. G. A., da Silva, M. A., dos Santos, L. O., & Beppu, M. M. (2011). Natural-based plasticizers and biopolymer films: A review. *European Polymer Journal*, *47*, 254–263.